Progress In Electromagnetics Research C, Vol. 149, 1-8, 2024

PIER C

(Received 11 September 2024, Accepted 14 October 2024, Scheduled 18 October 2024)

Bandwidth Enhancement of SIW-Fed Dielectric Rod Antennas via Tapered Grating

Shreya S. Menon[1,*], Khagindra K. Sood[2], Nalesh Sivanandan[1], and Supriya M. Hariharan[1]

[1]Department of Electronics, Cochin University of Science & Technology, Cochin, India
[2]Satcom and Satnav Applications Area, Space Applications Centre
Indian Space Research Organization, Ahmedabad, India

ABSTRACT: This study presents a technique to enhance the bandwidth of substrate-integrated dielectric rod antennas. The technique involves adding a tapered grating at the antenna input, which improves impedance matching. The tapered grating converts some of the guided mode fields into leaky mode fields, leading to improved matching and broader bandwidth. The effectiveness of this approach is demonstrated through simulations and measurements, showing significant bandwidth enhancement in both X-band and Ku-band designs. The design parameters and optimization process are detailed, and the scalability of the technique is confirmed by its successful application to different frequency bands. A design for X-band demonstrates the effectiveness of this technique, yielding a bandwidth of 40%. Additionally, the technique is applied to a previously reported Ku-band design, resulting in an improved bandwidth of 52%, up from 36%. The paper concludes that the proposed tapered grating is an effective approach to enhance the bandwidth of substrate-integrated dielectric rod antennas, particularly for medium or high-gain applications.

1. INTRODUCTION

Dielectric antennas offer several advantages over their metallic counterparts, primarily due to their compact size and superior gain performance. These antennas are typically lightweight and possess non-corrosive properties, making them suitable for a wide range of applications. Notably, they are effective in plasma diagnostics, millimeter-wave systems, and improving the performance of microwave reflector antennas. Additionally, dielectric antennas can be used as loads to modify the radiation pattern of metallic horns and serve as key elements in integrated circuits and phased array systems [1].

Dielectric rod antennas, in particular, are widely utilized in array configurations where closely spaced elements are necessary to avoid grating lobes [2–5]. These rods can be composed of a single dielectric material or include an outer layer with a lower dielectric constant to enhance performance [6–9]. Alternatively, hollow dielectric rods can be employed to achieve low sidelobe levels (SLL) [10]. Multilayer dielectric rod structures are advantageous as they concentrate electromagnetic energy within the inner core, minimizing the excitation of higher-order modes, and consequently, extending the antenna's operational bandwidth, with bandwidth ratios exceeding $4:1$ [9]. Dielectric rods are typically classified based on their cross-sectional shape — either rectangular or circular. The choice of waveguide used to feed the dielectric rod plays a critical role in determining the bandwidth of the antenna.

Dielectric rods also find extensive use in millimeter-wave applications that demand seamless integration with the chip itself [11–13]. While substrate-integrated dielectric rods have been explored, their bandwidth has been typically limited [14, 15]. This paper introduces a novel technique employing a tapered grating to substantially enhance the impedance bandwidth of these antennas. The concept of using a tapered grating for input matching was initially demonstrated in horn image guide leaky-wave antennas and later extended to dielectric horns for bandwidth improvement [16]. Both of these prior implementations involved printed antenna structures. The tapered grating functions by efficiently converting guided mode fields into leaky mode fields, thereby improving impedance matching. To the best of our knowledge, this paper presents the first application of a tapered grating to dielectric rod antennas.

The subsequent sections of this paper will delve into the working principle behind this technique, elaborate on the design parameters of a substrate-integrated dielectric rod antenna incorporating the proposed tapered grating, and present an X-band prototype showcasing simulation results, parametric analysis, and optimization. Furthermore, the efficacy of the tapered grating technique will be validated by applying it to a previously reported design, and measured results will be provided to substantiate the simulated findings.

2. WORKING PRINCIPLE

Dielectric rods, when being fed with a Substrate Integrated Waveguide (SIW), often exhibit poor impedance matching, which can degrade performance. To address this issue, tapered parallel strips are introduced at both the top and bottom of the structure, as highlighted in [17]. These strips serve a purpose: to allow some of the guided modes to leak progressively in the

* Corresponding author: Shreya S. Menon (shreyasmenon@cusat.ac.in).

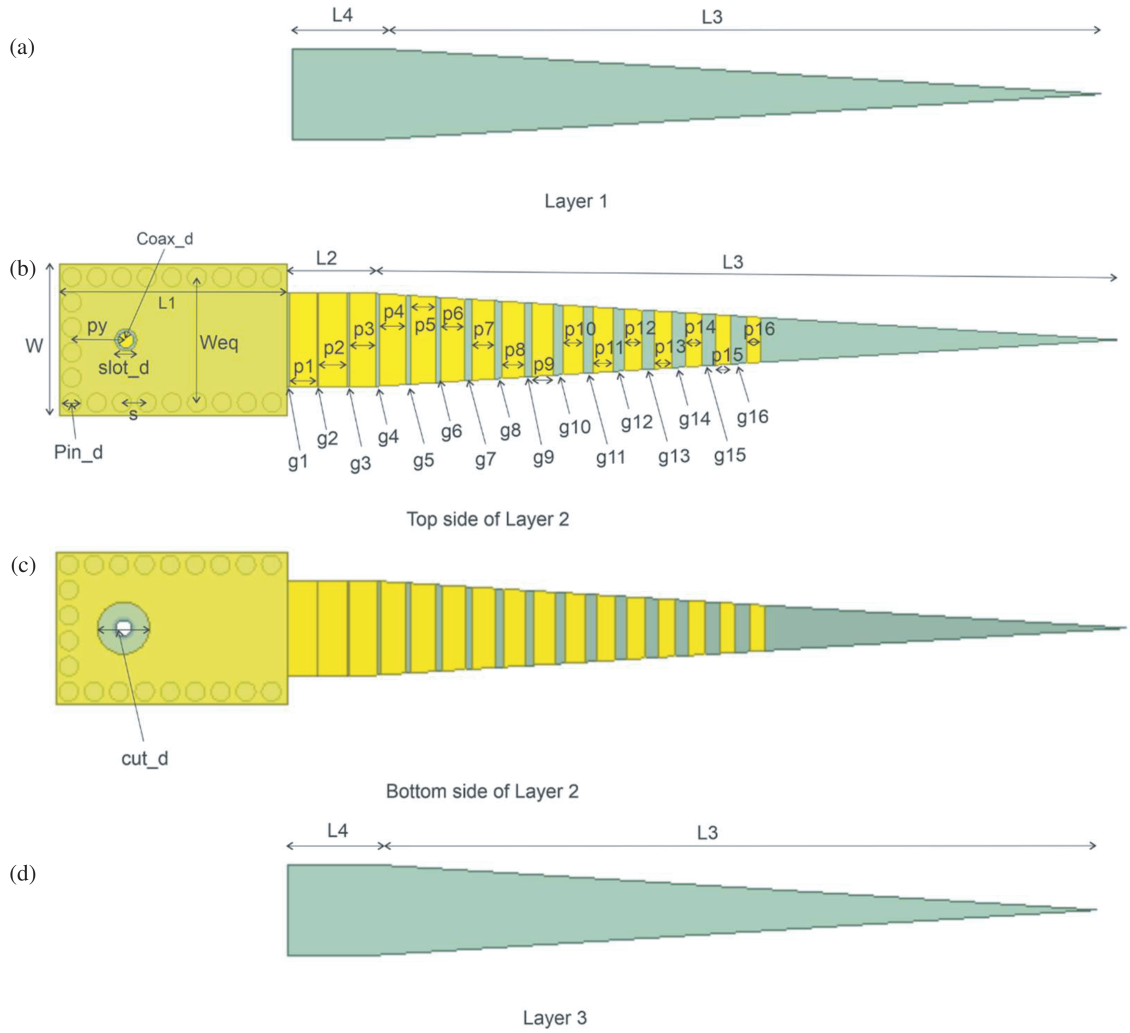

FIGURE 1. Configuration of dielectric rod antenna with the proposed tapered grating: (a) Layer 1, (b) Top side of Layer 2, (c) Bottom side of Layer 2, (d) Layer 3.

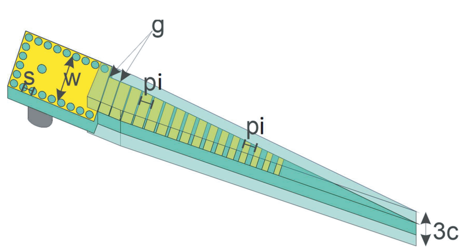

FIGURE 2. 3D view of dielectric rod antenna with the proposed tapered grating.

lateral direction, which improves the overall matching of the system.

In prior work [14], the approach utilized only two parallel strips of uniform dimensions to enhance matching. However, in this study, we introduce a more advanced method by incorporating 16 tapered parallel strips with progressively decreasing widths, as described in [17]. This refinement significantly improves the impedance matching compared to earlier designs and has been validated across multiple frequency bands, including X-band.

For the first time, this tapered leaky-wave technique has been applied to dielectric rods fed with SIW. One of the key aspects of this design is that the energy leakage is controlled, meaning that not all the energy is leaked in lateral direction. A portion of the guided wave reaches the tip of the dielectric rod, where it radiates outward. This dual-function design effectively combines the advantages of both guided and leaky wave radiation modes, leading to improved radiation performance and bandwidth.

3. DESIGN PARAMETERS

The proposed antenna design features a substrate-integrated dielectric rod with a tapered grating structure, aiming to enhance impedance matching and broaden bandwidth. The antenna comprises three dielectric layers, each tapered along one dimension while maintaining a uniform thickness in the other (see Fig. 1 and Fig. 2). The middle layer incorporates the tapered grating, which seamlessly extends from a substrate waveguide coax transition. The width of the grating elements progressively decreases, following a design equation that determines the width of the third and subsequent gratings based on an ini-

TABLE 1. Parameter values for the tapered grating design.

Parameter	Value (mm)	Parameter	Value (mm)	Parameter	Value (mm)	Parameter	Value (mm)
$g1$	0.107	$g2$	0.107	$g3$	1.89	$g4$	0.270
$g5$	0.352	$g6$	0.433	$g7$	0.515	$g8$	0.597
$g9$	0.678	$g10$	0.760	$g11$	0.841	$g12$	0.923
$g13$	1	$g14$	1.086	$g15$	1.168	$g16$	1.25
$p1$	2.25	$p2$	2.25	$p3$	2.17	$p4$	2.09
$p5$	2.01	$p6$	1.9	$p7$	1.84	$p8$	1.76
$p9$	1.68	$p10$	1.6	$p11$	1.52	$p12$	1.44
$p13$	1.35	$p14$	1.27	$p15$	1.19	$p16$	1.12

tial width ($wg0$), a progressive reduction in grating width (*step*), and the grating number (n).

$$wg\,(n) = wg0 - n * step \tag{1}$$

The grating pitch (pi) represents the distance between corresponding grating edges, and g denotes the gap between the first two gratings. The feed connector is strategically positioned at approximately a quarter-wavelength distance ($\lambda g/4$) from the shorted end. The exact position of the feed is subject to optimization during the design process. Additionally, the width W of the substrate-integrated waveguide (SIW) and the spacing s between the SIW pins are determined based on standard SIW design guidelines.

The initial dimensions for the radiator were derived using the design methodology specified in [14], ensuring consistency with prior work. For simplicity, the height of all three dielectric layers was maintained constant, denoted as c. The SIW dimensions were set to $W \times c$.

By introducing a taper in the grating, the design enhances impedance matching, promoting a smoother transition of electromagnetic waves. This taper gradually reduces the width of the grating to ensure efficient radiation and minimize reflections. The gap g and pitch pi are key parameters that control the behaviour of the leaky waves, optimizing both the impedance bandwidth and radiation characteristics.

This multi-layered and tapered configuration is crucial in improving the bandwidth, as the dielectric rod is capable of supporting both guided and leaky modes. The optimized design balances these modes to achieve enhanced performance, particularly in medium frequency bands like the X-band.

4. X-BAND PROTOTYPE

For X-band design, the chosen substrate material was Rogers RT/duroid 6006, which has a dielectric constant of 6.15. Each dielectric layer has a height of 2.54 mm. The initial grating parameters were derived from the design presented in [16], where a tapered grating was used in a horn antenna design. After running the optimization process (detailed in Subsection 4.4), the optimized parameter values for the X-band design were determined as follows: the initial grating width, wg, was set at 2.25 mm; the step size, which defines the progressive decrease in grating width, was set at 0.08 mm; the grating pitch pi was 2.357 mm; and the gap between the first two gratings, g, was set to 0.08 mm. These values are illustrated in Fig. 1 and detailed in Table 1.

4.1. Configuration and Design Specifications

The antenna is fed via a substrate-integrated waveguide (SIW) with dimensions of 10 mm by 2.54 mm. The spacing between the SIW pins was calculated using standard SIW design equations [18] and resulted in a value of 2 mm. The dielectric rod antenna maintains a constant width for the first 6 mm, after which it gradually tapers over a length of 60 mm, corresponding to the total radiator length as outlined in [14]. The full length of the antenna, from the feed to the tip, measures 84.5 mm.

In Fig. 1, the configuration of the dielectric rod antenna with the proposed tapered grating is illustrated, showing (a) Layer 1, (b) the top side of Layer 2, (c) the bottom side of Layer 2, and (d) Layer 3. Fig. 2 provides a 3D view of the antenna, highlighting the gradual tapering of the rod. This taper ensures efficient impedance matching and smooth radiation, with the energy progressively transitioning from the guided mode to radiating leaky-wave mode, optimizing performance across the entire X-band.

4.2. Simulation Results

The performances of the designed dielectric rod antenna, with and without the application of the tapered grating, were simulated and compared. The results clearly show that the tapered grating significantly improves the return loss of the antenna. Specifically, the return loss for the antenna without the grating is approximately -4 dB, which indicates relatively poor matching. In contrast, with the tapered grating, the return loss improves substantially, covering the entire X-band (8–12 GHz) with a bandwidth of 40% (see Fig. 3). This enhancement demonstrates the effectiveness of the tapered grating in achieving better impedance matching across a wide frequency range.

Additionally, the radiation pattern of the dielectric rod antenna equipped with the tapered grating reveals a well-defined and stable main lobe across the band of interest (see Fig. 4). This consistent radiation pattern indicates that the antenna maintains its directional characteristics effectively. The peak gain of the antenna also varies across the frequency band, with a maximum gain of 12 dBi at mid-band (around 10.6 GHz) and

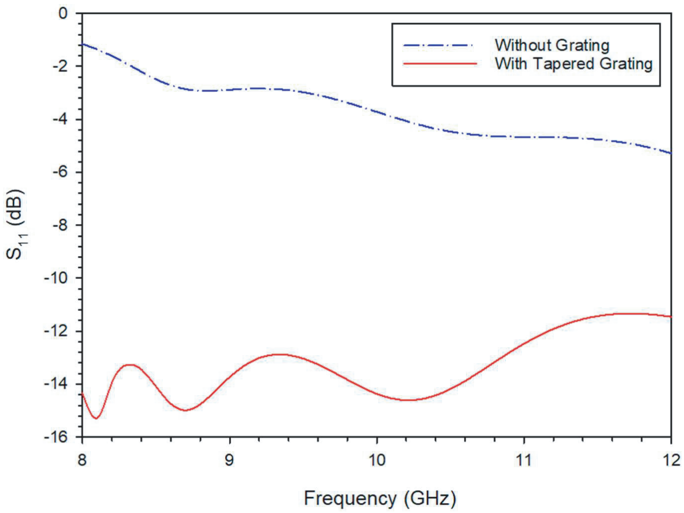

FIGURE 3. Return loss of dielectric rod with and without tapered grating.

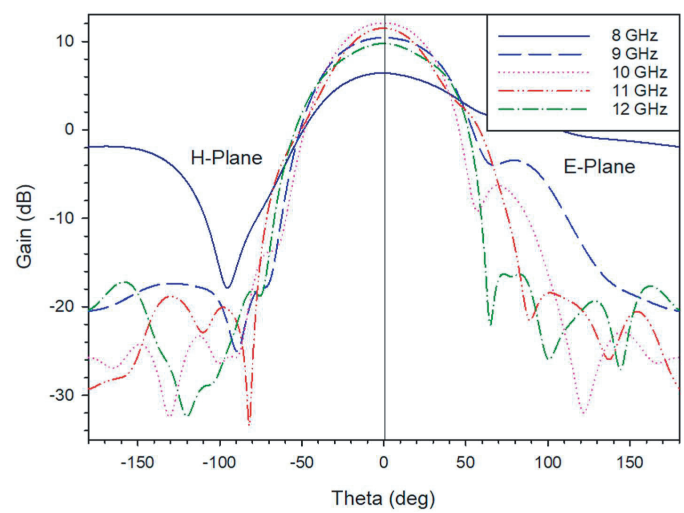

FIGURE 4. Radiation patterns of the dielectric rod with tapered grating.

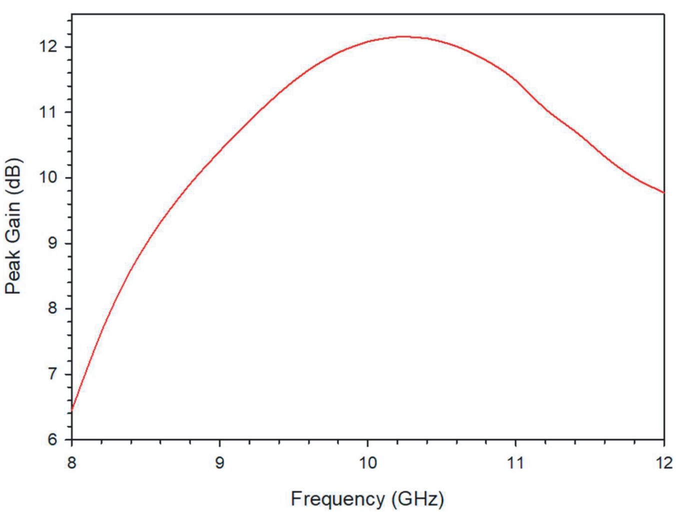

FIGURE 5. Peak gain versus frequency of dielectric rod with tapered grating.

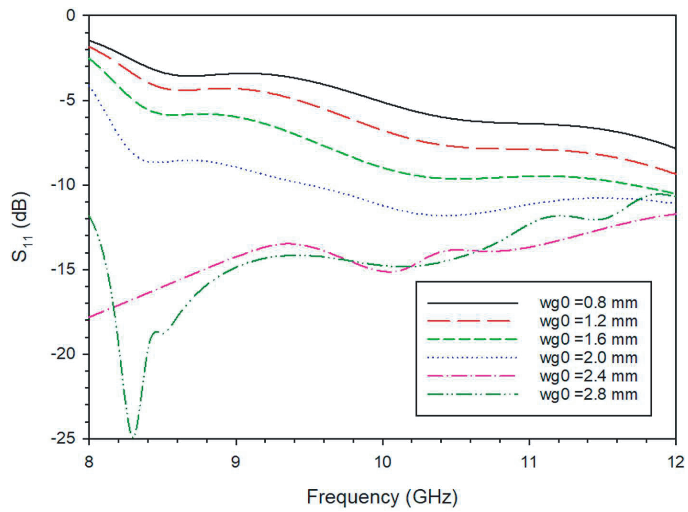

FIGURE 6. Variation of return loss versus changing the width of first two strips, $wg0$.

a minimum gain of greater than 6 dBi at the lower end of the frequency range (around 8 GHz) (see Fig. 5). These results confirm the capability of the proposed design to achieve both high gain and broad bandwidth, making it suitable for X-band applications.

4.3. Parametric Analysis

To further evaluate the performance and robustness of the design, a parametric study was conducted, examining the sensitivity of the antenna's return loss (S_{11}) with respect to key design parameters such as wg (initial grating width), g (gap between the first two strips), and step size (the progressive decrease in grating width).

- Effect of $wg0$: The return loss (S_{11}) decreases in the lower frequency range as $wg0$ increases, indicating better matching at lower frequencies. However, in the mid-frequency range, increasing $wg0$ causes S_{11} to increase slightly, showing a trade-off between low and mid-frequency performances (see Fig. 6).
- Effect of Gap g: The return loss initially increases and then decreases as the gap between the first two strips (g) increases (see Fig. 7). This behavior suggests an optimal gap size for achieving the best impedance matching, particularly at certain frequency bands.
- Effect of Step Size: The step size, which controls the progressive decrease in grating width, also influences S_{11}. In the lower frequency range, increasing the step size improves matching (decreasing S_{11}), while in the mid-frequency range, increasing the step size causes S_{11} to increase. However, in the upper frequency range, the step size has little to no effect on the return loss (see Fig. 8).

These parametric studies provide crucial insights into the behaviour of the antenna and allow for further optimization of the

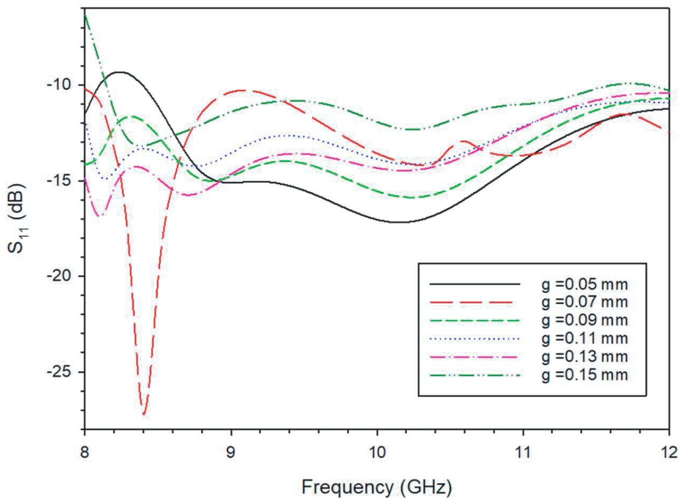

FIGURE 7. Variation of return loss versus changing gap between strips, g.

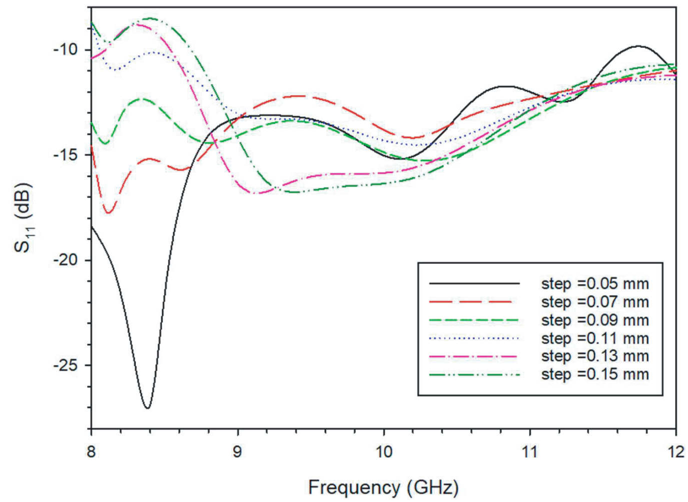

FIGURE 8. Variation of return loss versus changing step size, step.

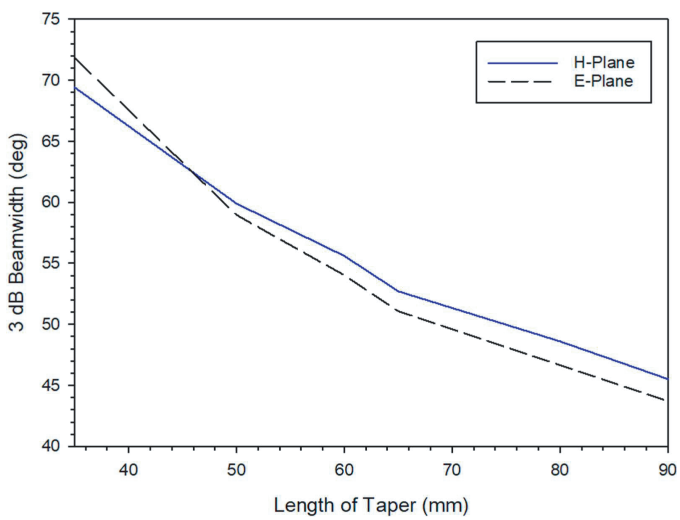

FIGURE 9. Variation of 3 dB beamwidth with varying length of taper.

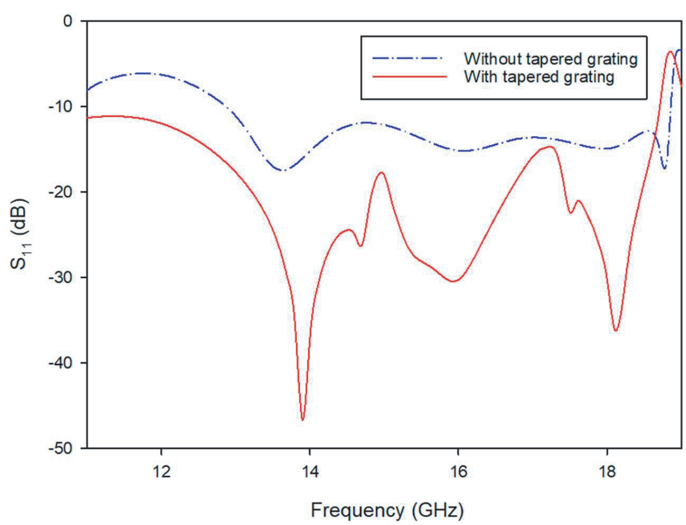

FIGURE 10. Return loss of dielectric rod with and without [14] tapered grating.

design based on the specific requirements of different applications.

4.4. Simulation Optimization

The parametric analysis can sometimes lead to suboptimal results, as it might converge on local minima rather than the global optimum with respect to the desired performance characteristics. To address this, a two-stage optimization process was implemented to ensure that the global minima, representing the optimal performance of the antenna, were achieved.

In the first stage, a **genetic algorithm** was employed for random optimization. Genetic algorithms are useful for exploring a wide solution space, especially in cases where the solution landscape contains many local minima. Following this, the second stage utilized **Sequential Non-Linear Programming (SNLP)**, a gradient-based optimization technique, to refine the results obtained from the genetic algorithm. Ansys Electronics Desktop was used for simulation of the design. It has inbuilt Optimization Techniques like GA (Genetic Algorithm) and SNLP. This two-step approach allowed for a more precise determination of the optimal dimensions for the tapered grating.

The key design parameters optimized in this process were the gap between the first two strips g, the grating pitch pi, and the step size of the tapered grating. The primary goal of this optimization was to maximize the impedance bandwidth across the targeted frequency range. By adjusting these parameters, the antenna's impedance matching and bandwidth performance were significantly improved.

However, a minor limitation of the proposed tapered grating design was identified: the requirement for a relatively long input-matching section. As the length of the taper increases, the 3 dB beamwidth of the dielectric rod antenna decreases (see

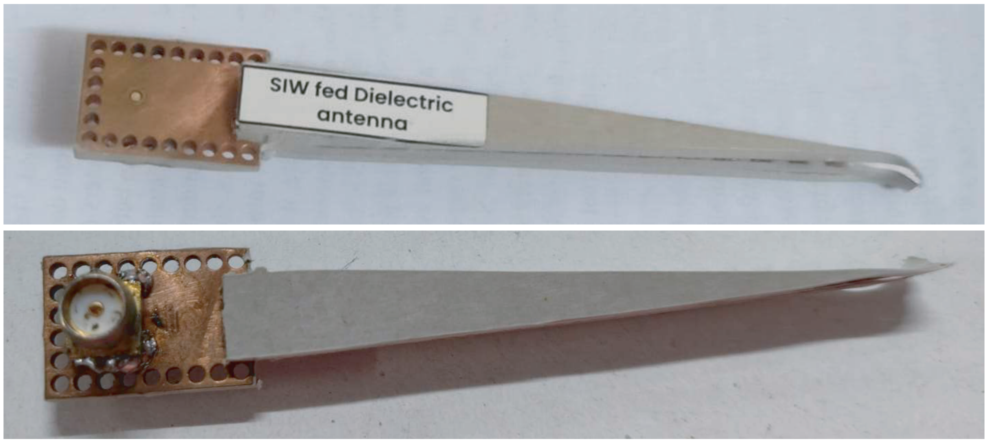

FIGURE 11. Fabricated dielectric rod with tapered grating.

Fig. 9). This creates a trade-off between the taper length and beamwidth. In cases where the radiator dimensions are constrained by far-field requirements, it may not be feasible to include the requisite number of tapered grating sections, which in turn limits the achievable bandwidth enhancement.

Consequently, this tapered grating technique is best suited for dielectric rod antennas designed for medium to high-gain applications, where the antenna dimensions allow for the inclusion of a sufficient number of grating sections to optimize bandwidth.

5. VERIFICATION OF PROPOSED TECHNIQUE

The proposed technique was validated by applying it to a previously reported design for a substrate-integrated dielectric rod antenna, published by Prasad and Biswas in 2016 [14]. The original design incorporated two metal strips as a simple grating, which were not tapered. In their study, the addition of these metal strips increased the antenna's impedance bandwidth from 2 GHz to 4.6 GHz.

To validate the effectiveness of the tapered grating introduced in this work, the same design [14] was simulated again, but this time with the addition of 14 tapered metal strips. The simulation was conducted in the Ku-band, and the widths of the third and subsequent gratings were determined using the initial width $wg0 = 1.665$ mm with a step size of 0.06 mm (as defined in Eq. (1)). The grating pitch was set to $pi = 1.745$ mm, while all other dimensions remained identical to the original design [14].

The comparison of the results (see Fig. 10) showed a significant improvement in the return loss with the tapered grating. Specifically, the -10 dB bandwidth was extended from 11 GHz to 18.7 GHz, increasing the bandwidth from 36% to 52%. This substantial improvement demonstrates the scalability and effectiveness of the proposed tapered grating technique when it is applied to passive radiating structures, further confirming its applicability to optimize Ku-band designs.

6. MEASUREMENT RESULTS & DISCUSSION

Due to the available fabrication standards, a minimum metal-to-metal spacing of 0.2 mm was required, whereas the original design used a spacing of 0.107 mm. Consequently, the design had to be re-optimized with a metal spacing greater than 0.2 mm for fabrication purposes. The prototype of the fabricated dielectric rod antenna with the tapered grating is shown in Fig. 11. The antenna's return loss (S_{11}), radiation pattern, and gain were measured at the Space Applications Centre, Indian Space Research Organization (ISRO), Ahmedabad, India, using a Vector

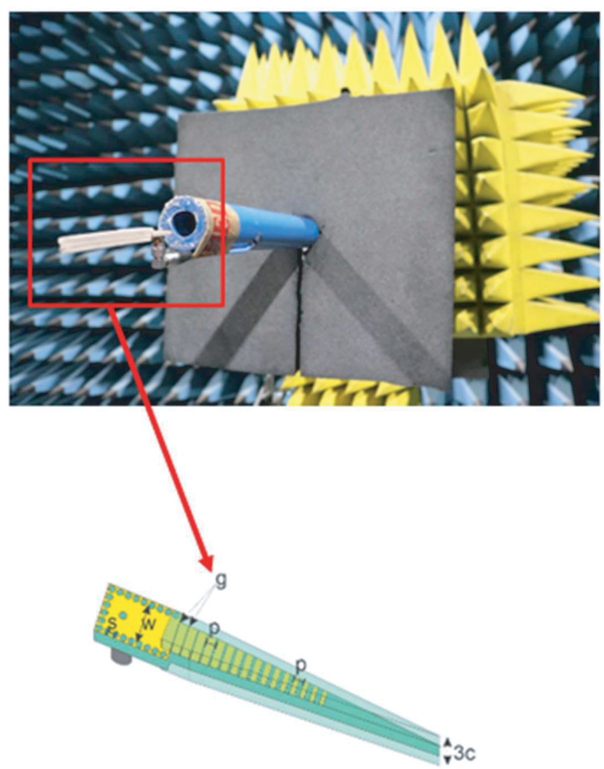

FIGURE 12. Measurement setup of X-band prototype.

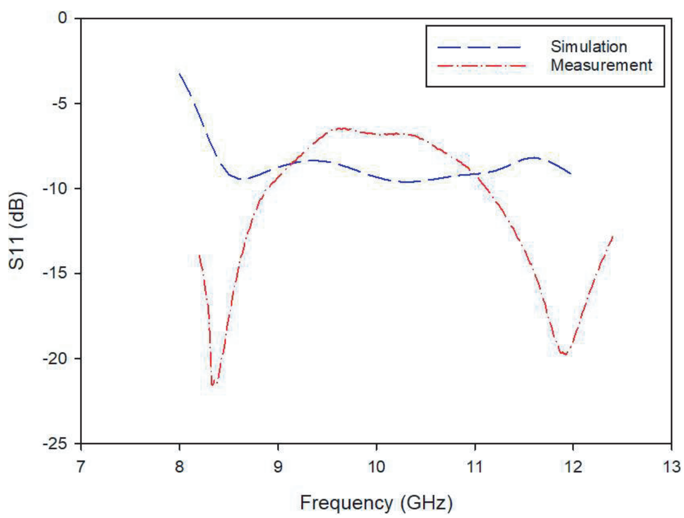

FIGURE 13. Return loss of dielectric rod with tapered grating.

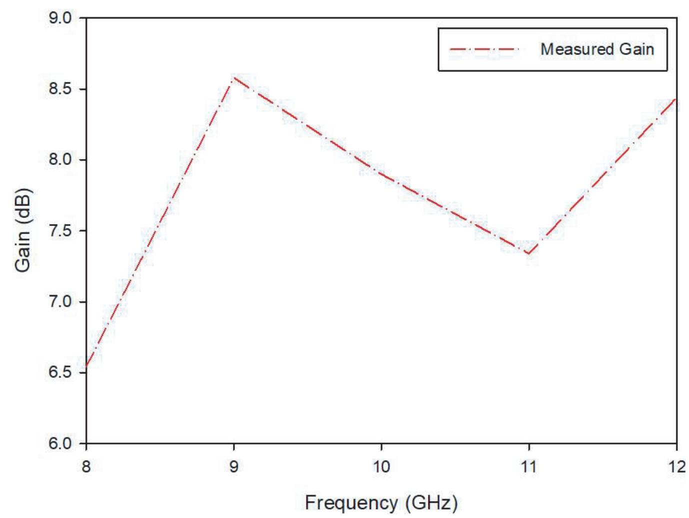

FIGURE 14. Measured gain of dielectric rod with tapered grating.

TABLE 2. Comparison table between recent published works and our results.

Work	Grating	Tapered Grating	Bandwidth	Band	Measured Gain
Slot fed Dielectric rod [19]	no	no	26%	Ku band	19dB
SIW fed Dielectric rod antenna (**This work**)	yes	yes	52%	Ku band	-
Yagi integrated dielectric rod antenna [20]	no	no	16.3%	X-band	17.3 dB
SIW fed Dielectric rod antenna (**This work**)	yes	yes	40%	X-band	~10 dB
[14]	yes	no	36%	Ku band	10dB

Network Analyzer (VNA) and an anechoic chamber setup, respectively. The measurement setup is shown in Fig. 12.

The measured S_{11} is compared with the simulated results in Fig. 13. Although the measured and simulated results exhibit a general agreement, some discrepancies may arise due to fabrication and soldering errors. The performance of the design is highly sensitive to parameters such as $wg0$, g, and step size, so even small variations between the simulated and fabricated designs can lead to differences in performance. Advanced fabrication technologies can help minimize the gap between the measured and simulated results, offering more precise alignment with the design specifications.

The measured gain of the antenna (see Fig. 14) remains above 6 dB across the band of interest, which is consistent with the simulated predictions. The radiation patterns of the antenna, plotted in Fig. 15, also align with the expected directional behaviour, validating the overall design and performance improvements achieved through the tapered grating.

With 1 oz Cu cladding, only 200 µm metal to metal spacing tolerance was achievable. Accuracy variation can easily mistune the antenna. Fabrication with maximum 50 µm spacing tolerance is required to properly compare the simulated and measured results. That is why there is a discrepancy between the simulated and measured values in Figs. 13, 14, and 15. The measured return loss near 11 GHz is less, and therefore, the measured gain is also affected as shown in Fig. 14. As the frequency increases, expected gain is higher as the electrical dimensions seen by the wave are more. But since the measured return loss around 11 GHz is less, the measured gain dips. The measured return loss can be expected to be low as the metal to metal spacing tolerance for fabrication achieved was around 200 µm.

Table 2 compares our work with recent works in dielectric antenna. We can see very well that the input impedance match achieved by our work is better than a few recent works. This work mainly focuses on return loss of the antenna and not gain.

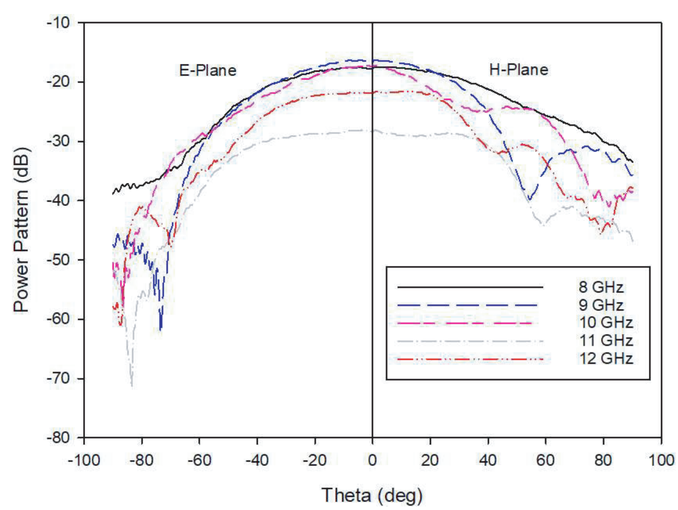

FIGURE 15. Measured radiation pattern of dielectric rod with tapered grating.

TABLE 3. Comparison between simulated and measured results.

	Simulated	Measured
Gain @ 10 GHz:	~11.5 dB	~7.9 dB
Beamwidth @ 10 GHz:	$55^\circ \times 56^\circ$	$48^\circ \times 49.5^\circ$

Gain may be improved with other techniques like increasing length of taper. Table 3 shows the comparison between simulated and measured results.

7. CONCLUSION

This study presents a novel tapered grating approach to significantly enhance the impedance bandwidth of a substrate-integrated waveguide-fed dielectric rod antenna. The design parameters were successfully optimized using a two-stage optimization routine, yielding an X-band prototype with a well-matched return loss across the entire band. The proposed technique was further validated by applying it to a previously reported Ku-band design [14], achieving a significant bandwidth improvement. While some gaps were observed between the measured and simulated results, these can be mitigated with more advanced fabrication technology. The results highlight the effectiveness of the tapered grating in enhancing antenna performance across multiple frequency bands, making it a promising solution for high-gain, broadband applications.

ACKNOWLEDGEMENT

The authors thank CSIR Emeritus Scientist Scheme for financially supporting this research.

REFERENCES

[1] Menon, S. S., D. D. Krishna, C. K. Aanandan, and S. K. Pathak, "Guided and leaky mode characteristics of solid dielectric horn: Analytical and numerical solutions," in *2020 IEEE International Symposium on Antennas and Propagation and North American Radio Science Meeting*, 279–280, Montreal, QC, Canada, Jul. 2020.

[2] Rivera-Lavado, A., S. Preu, L. E. García-Muñoz, A. Generalov, J. Montero-de Paz, G. Döhler, D. Lioubtchenko, M. Méndez-Aller, F. Sedlmeir, M. Schneidereit, *et al.*, "Dielectric rod waveguide antenna as THz emitter for photomixing devices," *IEEE Transactions on Antennas and Propagation*, Vol. 63, No. 3, 882–890, Mar. 2015.

[3] Pousi, J. P., D. V. Lioubtchenko, S. N. Dudorov, and A. V. Raisanen, "High permittivity dielectric rod waveguide as an antenna array element for millimeter waves," *IEEE Transactions on Antennas and Propagation*, Vol. 58, No. 3, 714–719, Mar. 2010.

[4] Nguyen, T. P., C. Pichot, C. Migliaccio, and W. Menzel, "Study of folded reflector multibeam antenna with dielectric rods as primary source," *IEEE Antennas and Wireless Propagation Letters*, Vol. 8, 786–789, 2009.

[5] Camblor, R., S. V. Hoeye, C. Vázquez, G. Hotopan, M. Fernández, A. Hadarig, and F. Las-Heras, "Submillimeter wave 8 × 1 antenna array with dielectric rods to improve the radiation pattern," in *2013 European Radar Conference*, 375–378, Nuremberg, Germany, Oct. 2013.

[6] Lugo, D. C., R. A. Ramirez, J. Wang, and T. M. Weller, "Low permittivity cladding to improve the performance of dielectric rod waveguides and dielectric end-fire antennas," in *2016 IEEE MTT-S International Microwave Symposium (IMS)*, 1–3, San Francisco, CA, USA, May 2016.

[7] Chung, J.-Y. and C.-C. Chen, "Two-layer dielectric rod antenna," *IEEE Transactions on Antennas and Propagation*, Vol. 56, No. 6, 1541–1547, Jun. 2008.

[8] Chen, C.-C., "UWB dielectric rod antenna designs," in *2013 7th European Conference on Antennas and Propagation (EuCAP)*, 758–759, Gothenburg, Sweden, Apr. 2013.

[9] Kazemi, R., A. E. Fathy, and R. A. Sadeghzadeh, "Dielectric rod antenna array with substrate integrated waveguide planar feed network for wideband applications," *IEEE Transactions on Antennas and Propagation*, Vol. 60, No. 3, 1312–1319, Mar. 2012.

[10] Kumar, C., V. V. Srinivasan, V. K. Lakshmeesha, and S. Pal, "Design of short axial length high gain dielectric rod antenna," *IEEE Transactions on Antennas and Propagation*, Vol. 58, No. 12, 4066–4069, Dec. 2010.

[11] Lugo, D. C., R. A. Ramirez, J. Castro, J. Wang, and T. M. Weller, "3D printed multilayer mm-wave dielectric rod antenna with enhanced gain," in *2017 IEEE International Symposium on Antennas and Propagation & USNC/URSI National Radio Science Meeting*, 1247–1248, San Diego, CA, USA, 2017.

[12] Trinh, T. N., J. A. G. Malherbe, and R. Mittra, "A metal-to-dielectric waveguide transition with application to millimeter-wave integrated circuits," in *1980 IEEE MTT-S International Microwave symposium Digest*, 205–207, Washington, DC, USA, 1980.

[13] Chen, C.-C., K. R. Rao, and R. Lee, "A new ultrawide-bandwidth dielectric-rod antenna for ground-penetrating radar applications," *IEEE Transactions on Antennas and Propagation*, Vol. 51, No. 3, 371–377, Mar. 2003.

[14] Prasad, C. S. and A. Biswas, "Planar excitation of dielectric waveguide antenna for broadband and high-gain application," *IEEE Antennas and Wireless Propagation Letters*, Vol. 16, 1209–1212, 2016.

[15] Prasad, C. S., A. Biswas, and M. J. Akhtar, "SIW slot fed circular dielectric rod antenna," in *2017 IEEE Applied Electromagnetics Conference (AEMC)*, 1–2, Aurangabad, India, Dec. 2017.

[16] Trinh, T. N., R. Mittra, and R. J. Paleta, "Horn image-guide leaky-wave antenna," in *1981 IEEE MTT-S International Microwave Symposium Digest*, 20–21, Los Angeles, CA, USA, Jun. 1981.

[17] Wang, L., M. Garcia-Vigueras, M. Alvarez-Folgueiras, and J. R. Mosig, "Wideband H-plane dielectric horn antenna," *IET Microwaves, Antennas & Propagation*, Vol. 11, No. 12, 1695–1701, 2017.

[18] Xu, F. and K. Wu, "Guided-wave and leakage characteristics of substrate integrated waveguide," *IEEE Transactions on Microwave Theory and Techniques*, Vol. 53, No. 1, 66–73, Jan. 2005.

[19] Saffold, G. L. and T. M. Weller, "Dielectric rod antenna array with planar folded slot antenna excitation," *IEEE Open Journal of Antennas and Propagation*, Vol. 2, 664–673, 2021.

[20] Nasir, M., Y. Xia, M. Jiang, and Q. Zhu, "A novel integrated Yagi–Uda and dielectric rod antenna with low sidelobe level," *IEEE Transactions on Antennas and Propagation*, Vol. 67, No. 4, 2751–2756, Apr. 2019.